

Tensile and flexural behavior of synthetic and hybrid natural fiber composites for lightweight applications

Karthikeyan Ramachandran  | Mohammed Khan | R. A. Tharuja Perera |
Doni Daniel Jayaseelan

Department of Aerospace and Aircraft Engineering, Kingston University, London, UK

Correspondence

Karthikeyan Ramachandran and Doni Daniel Jayaseelan, Department of Aerospace and Aircraft Engineering, Kingston University, Roehampton Vale Campus, London SW15 3DW, United Kingdom.
Email: k1825123@kingston.ac.uk and d.daniel@kingston.ac.uk

Abstract

The growing demand for lightweight and sustainable materials has driven research into hybrid composites that combine synthetic and natural fibers. This study aims to investigate the tensile and flexural behavior of carbon fiber (CF) and glass fiber (GF) composites, alongside hybrid composites incorporating flax and hemp fibers. The composites were fabricated using the vacuum bagging technique, ensuring uniform fiber distribution and optimized mechanical properties. Experimental results revealed that CF composites exhibited the highest ultimate tensile strength (~ 550 MPa), with failure dominated by matrix cracking and fiber breakage due to their inherent brittleness. GF composites, while having a lower tensile strength (~ 450 MPa), demonstrated greater ductility, attributed to fiber pull-out and matrix cracking. Hybrid composites (H1), combining CF and GF, showed intermediate tensile strength (~ 500 MPa), reflecting mixed failure modes. In contrast, natural fiber composites (FH and H2) displayed significantly lower strengths (~ 150 – 200 MPa) due to weaker fiber-matrix interactions and moisture sensitivity. Despite their lower strength, hybrid composites provided a balance between mechanical performance and sustainability, making them a promising alternative for lightweight structural applications in automotive, aerospace, and eco-friendly engineering. These findings highlight the potential of hybrid composites in reducing environmental impact while maintaining structural integrity, offering a viable solution for next-generation sustainable materials.

Highlights

- CF, GF, H1, FH, and H2 composites were prepared through vacuum bagging.
- CF showed strength (~ 550 MPa) with brittle failure; GF was ductile and moderate.
- H1 hybrids combined CF and GF for balanced performance at ~ 500 MPa.
- Natural fiber composites prioritize sustainability with lower strength.
- H2 hybrids offer a mix of eco-friendliness and improved durability.

This is an open access article under the terms of the [Creative Commons Attribution](https://creativecommons.org/licenses/by/4.0/) License, which permits use, distribution and reproduction in any medium, provided the original work is properly cited.

© 2025 The Author(s). *Polymer Composites* published by Wiley Periodicals LLC on behalf of Society of Plastics Engineers.

KEYWORDS

composites, natural fibers, tensile behavior, flexural strength, finite element approach (FEA)

1 | INTRODUCTION

The use of composite materials has been rapidly expanding in industries such as aerospace, space exploration, and transportation due to their superior specific strength and stiffness compared to conventional materials.^{1–4}

Carbon fiber reinforced polymer (CFRP) composites, in particular, now account for over 50% of the structural components in aircraft, owing to their cost-effectiveness and lower manufacturing expenses compared to metals and alloys.¹ For example, Boeing 787 Dreamliner contains approximately 23 tons of carbon fiber composites in its structure.⁵ However, the increased use of carbon fiber-reinforced composites has contributed to a 30% rise in greenhouse gas emissions from manufacturing processes and 44% of CO₂ emissions from industrial sources.⁶ Hybrid composites have emerged as a promising alternatives^{7,8} to address these sustainability challenges. Their applications have expanded significantly due to their advantages, including flexibility, cost-effectiveness, and recyclability.^{9,10} Beyond having properties similar to carbon fiber composites, biocomposites exhibit notable mechanical properties.¹¹ For instance, Yan et al. demonstrated that flax-based hybrid composites showed superior specific absorbed energy and compressive force efficiency compared to conventional metals in damping applications, making them a viable option for crashworthy structures.¹² Extensive research continues to explore the potential of hybrid composites in aerospace and automotive industries.^{13–15}

Furthermore, global commitment to achieving net-zero emissions has been steadily growing, with numerous countries implementing declarations and governance measures. However, despite these efforts to mitigate global warming, carbon-based emissions from industries and transportation have increased by approximately 60%, making it challenging to limit the rise in global temperatures to 1.5°C.^{16,17} Such policies and restrictions aimed at reducing carbon-based material waste have led to intensified research on naturally available materials that are both low-cost and renewable, contributing to the development of hybrid composites.^{18,19} These composites are engineered to exploit the advantages of different fibers, allowing for tailored properties.²⁰ The combination of fibers enables the optimization of properties such as tensile strength, impact resistance, stiffness, and thermal stability.²¹ For example, natural fibers like flax, jute, hemp, and sisal offer the advantages of biodegradability, low density, and

cost-effectiveness. However, their relatively low mechanical properties compared to synthetic fibers limit their applications.^{7,22} To overcome these limitations, natural fibers are often combined with synthetic fibers such as glass or carbon fibers, which provide higher strength and stiffness.

The use of natural fibers in hybrid composites also helps reduce the overall environmental footprint, as synthetic fibers are energy-intensive to produce and non-biodegradable.^{17,23,24} Additionally, hybrid composites have been shown to exhibit improved fatigue resistance and damping behavior compared to conventional composites, making them ideal for dynamic applications.²⁵ However, research on hybrid composites remains limited in terms of their failure behavior and water absorption index, with only a few studies exploring their full potential.^{15,25} This work aims to evaluate the mechanical properties of synthetic, natural, and hybrid composites fabricated using the vacuum bagging process and understand their failure mechanisms for future applications.

2 | MATERIALS AND METHODS

2.1 | Materials

A non-woven hemp mat with an areal weight of 100 g/m² and a thickness of 0.3 mm, along with a twill-woven flax cloth with an areal weight of 200 g/m² and a thickness of 0.3 mm, was sourced from Easy Composites, UK. Additionally, a carbon fiber twill fabric with an areal weight of 210 g/m² and a thickness of 0.3 mm, as well as a non-woven glass fiber mat with an areal weight of 280 g/m² and a thickness of 0.3 mm, were obtained from the same supplier. LB2 Epoxy laminating bio-resin was chosen due to its reduced environmental impact.

2.2 | Preparation of composites

The composites were fabricated using the vacuum bagging technique with a hand lay-up method. The mats/cloths were manually laid, followed by the resin impregnation. Hand rollers were used to ensure optimal interaction between the fibers and the matrix, promoting uniform resin distribution and achieving the desired thickness (3 mm). A compression load of 5 MPa was

TABLE 1 Nomenclature and number of layers on composites.

Nomenclature	Number of Layers
CF	10
GF	10
H1 (CF + GF)	10 (5 CF + 5 GF)
FH (Flax + Hemp)	10 (5 Flax + 5 Hemp)
H2 (Flax + Hemp + CF + GF)	10 (3 Flax + 3 Hemp + 2 CF + 2 GF)

applied for 20 minutes before the heat treatment. The prepared mold was covered using a breathable resin and placed in a flexible airtight envelope and the vacuumed. The mold was then sealed inside a flexible breathing bag and vacuumed. The composites were subsequently cured at 150°C for 3 hours. The woven layers were oriented at 0° to maintain consistency with the twill weave pattern, ensuring that the material properties remained unaffected. After curing, the composites were cut into desired shapes for mechanical studies using water jet cutting. Table 1 provides the nomenclature and number of layers for the manufactured composites.

2.3 | Mechanical properties and characterization

The water absorption test of composites was carried out as per ASTM D570 by measuring the weight gain of the specimen after immersion in water for 24 hrs. The samples were dried in an oven (Carbolite) at 60°C for 24 hrs to remove any existing moisture. After cooling in a controlled desiccator, the initial weight (W_0) is recorded. Then the specimens are then fully submerged in distilled water at room temperature for 24 hrs. After 24 hrs, the specimens are removed, wiped with a dry cloth to remove surface moisture, and immediately weighed (W_1) using a precision balance. The percentage of water absorption is calculated using Equation (1) where W_0 and W_1 are dry and wet sample weights respectively.

$$\text{Water Absorption (\%)} = \frac{W_1 - W_0}{W_0} \times 100 \quad (1)$$

Tensile tests were performed at room temperature using a Zwick/Roell Z050 Universal Testing Machine at Kingston University, operating at a crosshead speed of 2 mm/min. The machine was equipped with a 10 kN load cell and an integrated extensometer for accurate strain measurement. Tensile test specimens were prepared by water jet cutting from the composite sheets, following ASTM D3039 standards, with dimensions of 250 mm in

length, 25 mm in width, and 3 mm in thickness. Similarly, the flexural properties of the composites were evaluated using a three-point bending test in accordance with ASTM D7264. Rectangular specimens measuring 150 mm in length, 13 mm in width, and 3 mm in thickness were also prepared via water jet cutting. The same Zwick/Roell Z050 Universal Testing Machine, operating at a crosshead speed of 2 mm/min, was used for the three-point bending tests. The failure regions of the composites were examined using a microscopic approach through scanning electron microscopy (SEM) with a Zeiss EVO50 at Kingston University, London. To prepare the fractured areas for SEM analysis, the failed regions were carefully resized via water jet cutting to ensure they fit within the microscope chamber. Additionally, the resized samples were coated with a ~20 nm layer of Au/Pd nanoparticles using sputter coating to enhance their electrical conductivity, preventing charge build up, resulting in improved imaging quality.

Finite element analysis (FEA) was conducted using Ansys 19.2 to validate the experimental results. The composites were modeled utilizing the Composite Modeler, and a static structural analysis was performed with a fine quadratic mesh size of 0.01 mm to ensure accurate stress and deformation predictions. For the tensile test simulation, boundary conditions were applied by fixing one end of the specimen while a displacement of 2 mm/min was imposed on the opposite end. In the three-point bending simulation, two mid-span supports were fixed, and a displacement of 2 mm/min was applied at the midpoint of the specimen. Key outputs, including total deformation and equivalent stress distribution, were analyzed and compared with the experimental results to assess the model's accuracy and reliability.

3 | RESULTS AND DISCUSSION

3.1 | Water absorption

Figure 1 presents the water absorption rates of various composite materials, including CF, GF, FH, and hybrid composites (H1, and H2). From Figure 1, it is evident that CF exhibits the lowest water absorption at 4%, followed by H1 (4.8%) and GF (5.4%). The natural fiber-based composites FH and H2 show higher water absorption levels, with FH recording the highest value at 8.5% and H2 at 6.2%. The lower water absorption of the CF might have been due to the hydrophobic nature of carbon fibers and their resistance to moisture penetration.²⁶ Likewise, GF composites, which showcase higher absorption than CF which might have been attributed to the moisture absorption nature of glass fibers due to their hydrophilicity.²⁷ This might be a similar case for hybrid synthetic composites,

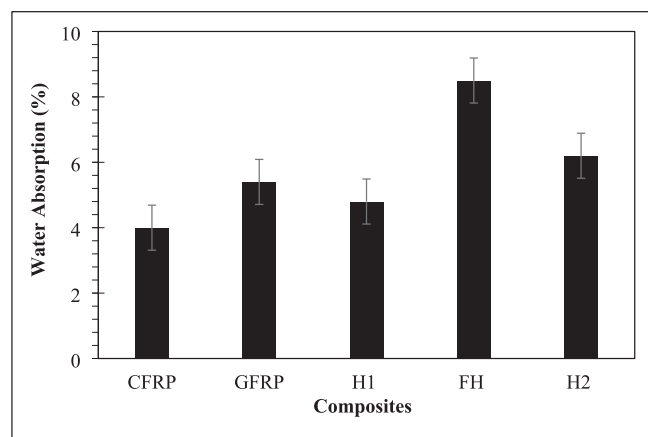


FIGURE 1 Water absorption properties of vacuum-bagged fabricated composites.

which should increase water absorption due to the moisture absorption behavior of glass fibers. On the other hand, natural composites (FH) indicate the highest water absorption rate due to their inherent hydrophilicity. Likewise, hybrid composites, which combine natural and synthetic materials, also had higher water uptake, which might have depended on the composition of natural fibers, which were hydrophilic. Furthermore, hybrid composites, due to their weaker interfacing bonding in woven composites, caused a reduced water absorption rate compared to the fiber-based structures, which is similar to findings reported in previous studies.^{28,29}

Furthermore, the presence of moisture on the composites significantly affects the mechanical integrity of the composites by degrading their mechanical properties by weakening the polymer matrix due to hydrolysis, which reduces its ability to transfer stress to the reinforcing fibers. Additionally, moisture disrupts the fiber-matrix interface, diminishing the bond strength and leading to reduced load-bearing capacity and premature failure.³⁰ This effect is particularly pronounced in composites using natural fibers like flax and hemp, which are inherently hydrophilic and absorb moisture readily. As a result, tensile and flexural strengths decrease, compromising the material's overall performance. Also, moisture-induced swelling and microcracking in the matrix can create pathways for further water ingress, accelerating degradation.³¹ In synthetic composites, such as carbon fiber (CF) and glass fiber (GF), the impact is less severe but still notable, particularly with prolonged exposure to humid environments.³²

3.2 | Tensile strength

The stress-displacement graph plotted in Figure 2 reports the tensile stress of different fabricated composites. Both

GF and H1 display similar trends, with a nearly linear increase in the stress. GF reaches a maximum stress of ~450 MPa, whereas H1 attains a higher peak stress of ~500 MPa, suggesting higher tensile strength. CF demonstrates the highest tensile stress, peaking at 550 MPa, indicating that the composite can endure high stress. In contrast, FH and H2 show significantly lower stresses of around 150 MPa and 200 MPa, respectively. By observing the tensile stress exhibited by the composites, it can be said that GF and H1 are in line with existing research on fiber-reinforced composites.²⁹ Both GF and H1 showcased moderate stress and stiffness, which aligns with various releases and highlights the strength-to-weight ratio of glass composites.³³ CF, on the other hand, displayed superior tensile stress consistent with the extensive literature documenting the high strength, toughness, and resilience of carbon fiber composites, making them suitable for demanding applications in aerospace and automotive sectors.^{34,35} The CF stress curve demonstrates high stress and substantial deformation before failure, underscoring carbon fiber's reputation for excellent load-bearing capacity and fracture toughness. However, the natural fiber-reinforced composites FH and H2 indicated a lower stress, which might have been attributed to inadequate fiber-matrix interaction or suboptimal fiber hybridization. This inadequate fiber matrix bonding could limit load transfer, leading to reduced mechanical performance.³⁶

On the other hand, H2 composite strength was influenced by the volume fraction of synthetic fibers incorporated. The hybridization of H2 with synthetic fibers enhanced its tensile strength and stiffness as the inherent weaknesses of natural fibers were improved. This sandwiching of synthetic fibers into natural fibers through ply-blocking improves the composite's moduli.³⁷ In this configuration, natural fibers provide initial compliance under tensile loads, while synthetic fibers resist deformation, leading to enhanced stiffness. Reducing the interface between natural and synthetic fibers further benefits stiffness, as it minimizes the potential for weak bonding. Also, fibers oriented to the load direction introduce an in-plane shear condition, where fibers tend to pull out under stress, reducing the maximum achievable strength for a fiber volume fraction.

The SEM images of the fracture surface of the post tensile study are illustrated in Figure 3. Figure 3A provides a cross-sectional view of CF composites that exhibit distinct signs of fiber pullout and debonding. The clean and elongated fiber surfaces illustrated in Figure 3A suggest a weak fiber-matrix adhesion, which may lead to fiber pull-out and debonding along the orientation of the fibers, which also limits the stress transfer from the matrix to the fibers, resulting in failure. Furthermore, delamination between fiber layers can intensify these

FIGURE 2 Stress vs. displacement curve for vacuum-bagged composites.

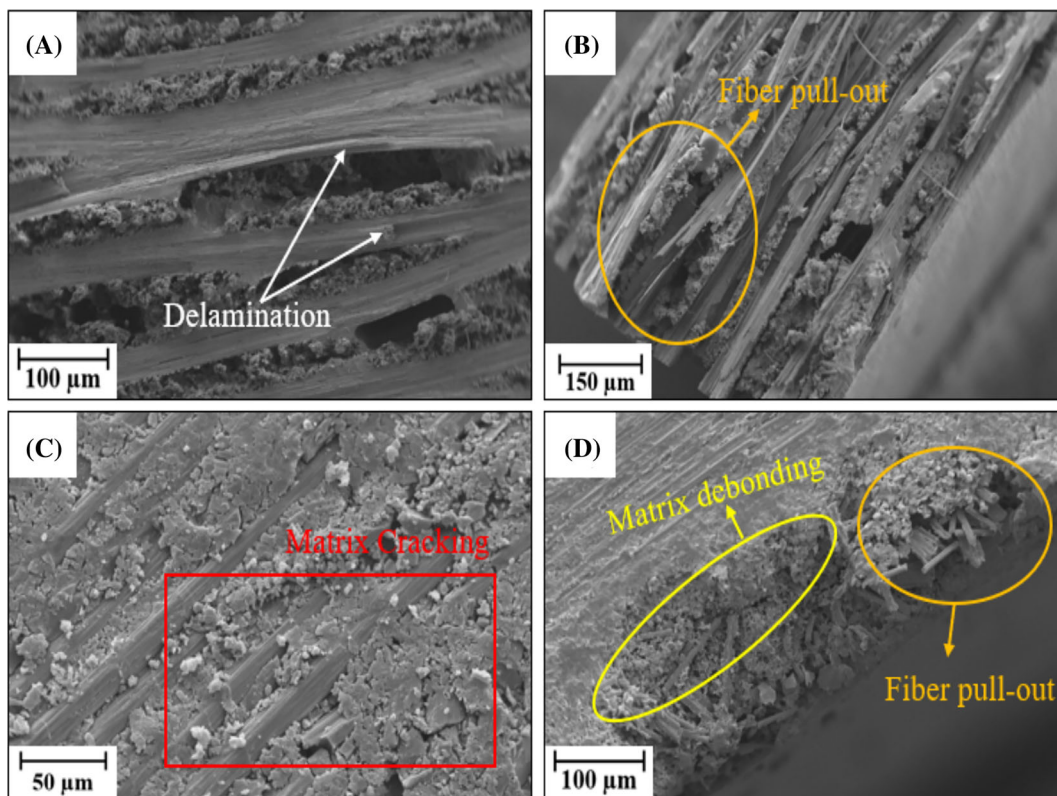
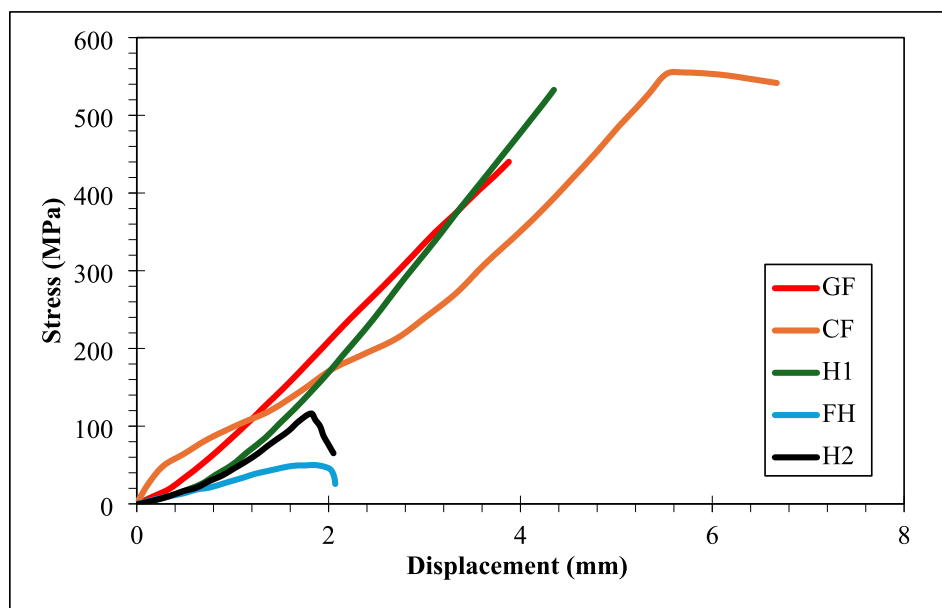


FIGURE 3 SE microscopic images of fractured areas (A) CF composite, (B) GF composite, and (C & D) H1 composite post tensile study.

issues, leading to reduced composite strength.^{35,38,39} Similarly, GF composites reported in Figure 3B indicate signs of brittle fracture due to the breakage of the fibers rather than fiber pull-out. This might have been due to the brittle nature of GF composites compared to the CF. The GF composites showcased fiber fractures into shorter lengths,

indicating a lack of plastic deformation prior to failure, which might have been attributed to maximum energy absorption by fibers rather than the matrix.^{40,41}

From Figure 3C,D, it can be observed that hybrid composite (H1) made from CF/GF composites displayed a mixed failure mode, which might be attributed to the

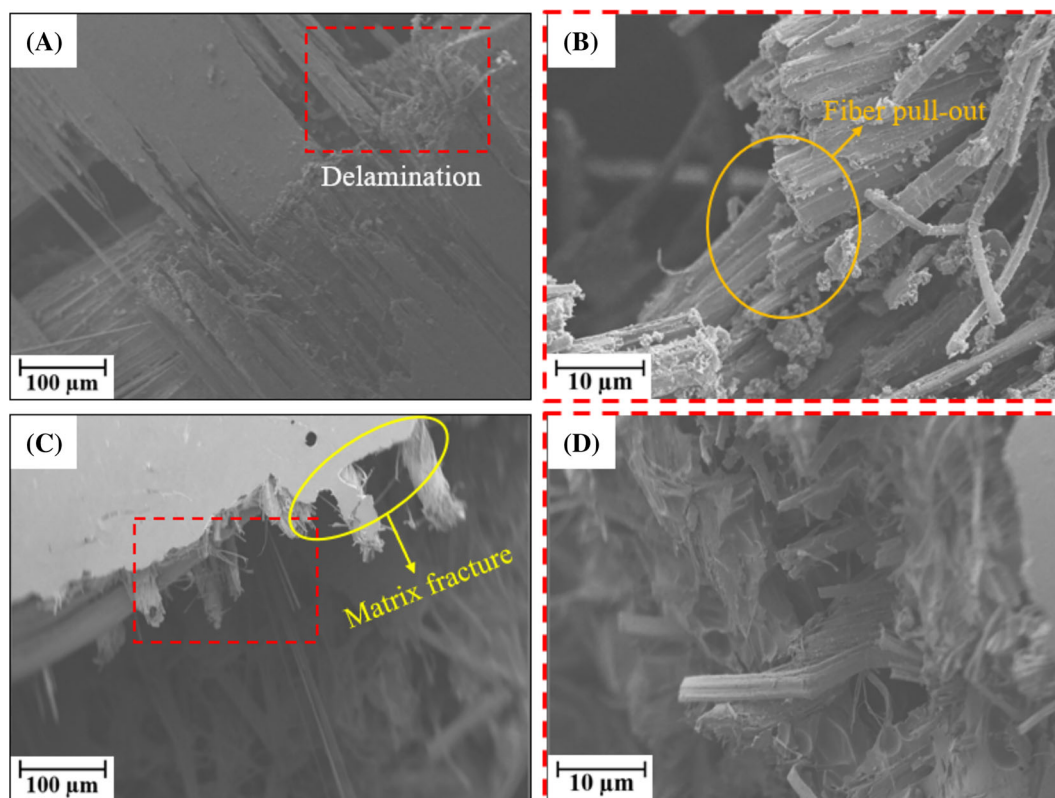


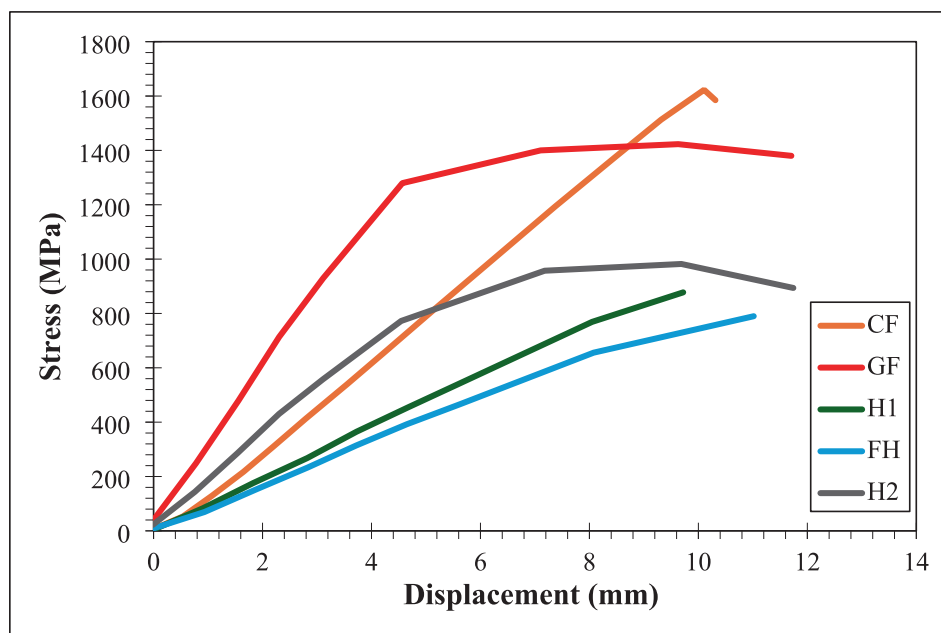
FIGURE 4 SE microscopic images of fractured areas (A, B) FH composite and (C, D) H2 composites post tensile study.

distribution and arrangement of CF/GF layers in the fabrication. The failure modes and mechanical properties of H1 composites were highly influenced by the interfacial bonding between the fibers and the matrix, as well as the inherent characteristics of the fibers. In this case, H1 composites demonstrated fiber pull-out due to a weak fiber-matrix interface, as illustrated in Figure 3C, and fiber fracture owing to the brittle nature of glass fibers, as reported in Figure 3D. This combined fracture behavior reduces its mechanical properties, resulting in lower tensile stress compared to CF but higher than GF. The combination of these fiber behaviors contributes to a unique failure mechanism that results in reducing the performance of the H1 composite. Such a failure mode is uncommon in hybrid composites, where delamination or matrix cracking typically dominates due to the mismatch in stiffness or thermal expansion between layers.⁴² The predominance of fiber-driven failures in this hybrid system can be attributed to the specific arrangement of CF and GF layers, as well as their woven structures.⁴³ The fiber architecture may have facilitated stress redistribution in a way that exposed the limitations of the individual fibers rather than causing interfacial delamination or matrix failure.⁴³

Figure 4 illustrates the failures of the natural fiber (FH) composites and hybrid (H2) composites post-tensile

study. Figure 4A,B reveals that the FH composites underwent significant fiber pull-out and matrix cracking, which is attributed to the weaker fiber-matrix interfacial bonding on the natural fibers.⁴⁴ The weaker interfacial bonding in the FH composites may lead to the detachment of fibers from the matrix, as observed in Figure 4B along with fracturing.¹⁴ The rough and fibrous texture of the pulled-out fibers indicates their ductile behavior, which allows for more energy absorption before final failure.^{45,46} This behavior aligns with various research where flax and hemp fibers are noted for their high strain-to-failure, making them effective in delaying crack propagation during tensile stress.^{5,8,14} On the contrary, Figure 4C,D reports the failures in H2 composites, which displayed a mixed failure mechanism. The brittle fracture behavior of glass and carbon fibers is evident, marked by clean breaks and matrix splitting, while the natural fibers exhibit more pronounced fiber pull-out, i.e., ductile behavior.⁴⁷ The presence of both ductile and brittle failures reflects the synergistic nature of the hybrid composites. The inclusion of natural fibers such as flax and hemp helps improve toughness and impact resistance, while the glass and carbon fibers contribute stiffness and strength. The hybridization of the composite leads to a more balanced mechanical response based on the composition

FIGURE 5 Flexural strength of the composites prepared via the vacuum bagging method.



of natural and synthetic composites.⁴⁸ In the case of H2 composites, the flax and hemp material was about 60%, which influenced the tensile strength and resulted in a drop in strength compared to other composites.

3.3 | Flexural strength

The flexural strength curve of vacuum bagged composites is illustrated in Figure 5. The synthetic fibers of carbon (CF) and glass (GF) composites exhibited the highest flexural strength, peaking at ~1620 MPa and ~1380 MPa, respectively. However, the combination of carbon and glass fiber (H1) composites indicated a stress of ~982 MPa, which was a drop of ~39% and ~28% compared to true synthetic fiber composites. This reduction in strength, relative to pure CFRP and GFRP, suggests that hybridization introduces trade-offs, as the load-sharing between the two fiber types might not be fully optimized. This steep higher stress for all three synthetic fiber composites indicates their superior stiffness and load-bearing capacity due to their high modulus of elasticity and excellent load transfer between fibers and matrix.⁴⁹ On the contrary, FH composites showcased lower flexural strength around ~780 MPa, reflecting the impact of natural fibers which generally have lower mechanical properties than synthetic fibers and likely contribute to reduced performance.⁵⁰ Likewise, H2 composites also showcased lower flexural strength (~870 MPa) which was about 10% higher than FH composites and might

have been influenced by the composition of flax and hemp layers despite the presence of CF and GF layers.

The SEM images reported in Figure 6 illustrate the fractured surfaces of CF and GF composites following a three-point bending test. Figure 6A reveals that the failure of CF composites was characterized by a brittle fracture with a clean, flat breakage of fibers with minimal matrix cracking, indicating that the carbon fibers withstood most of the load before failure. The sharp fiber fracture surfaces suggest high flexural strength but low strain tolerance, typical of CF composites in flexural tests. Brittle fracture is common in CF composites under bending due to their high stiffness and low elongation at break.⁵¹ Figure 6B illustrates matrix cracking on the surface of a CF composite. The image reveals the initiation and propagation of matrix cracks along the surface of the composite, which typically occurs due to stress concentration at weak points in the resin matrix, leading to brittle fracture of the matrix before significant fiber failure. This brittle nature reduces the load-carrying capacity of the composite as the cracks propagate through the matrix and eventually result in fiber-matrix debonding.⁵²

Figure 6C,D displays the fracture behavior of GF composites, characterized by a combination of fiber pull-out and matrix cracking. In Figure 6C, the fractured matrix surface exhibits roughness, indicating significant fiber-matrix debonding. This rough matrix surface is a result of the ductile nature of glass fibers, which possess a high strain-to-failure property.⁵³ The stress from the bending test induced separation at the fiber-matrix interface, forming distinct shear planes, which ultimately led

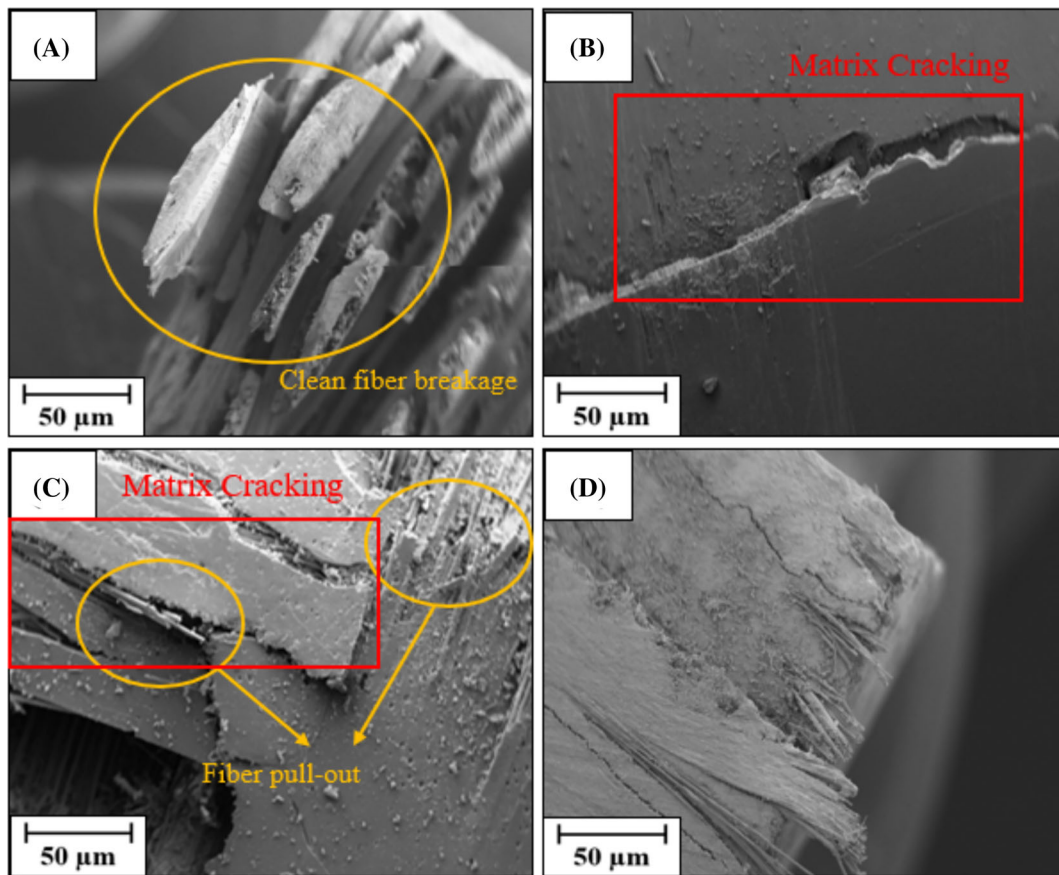


FIGURE 6 SE Images of fractured area post three-point bending test of (A) cross section of the CF, (B) fracture in the matrix of CF, (C) matrix fracture on GF, and (D) fiber pull-out in the GF composites.

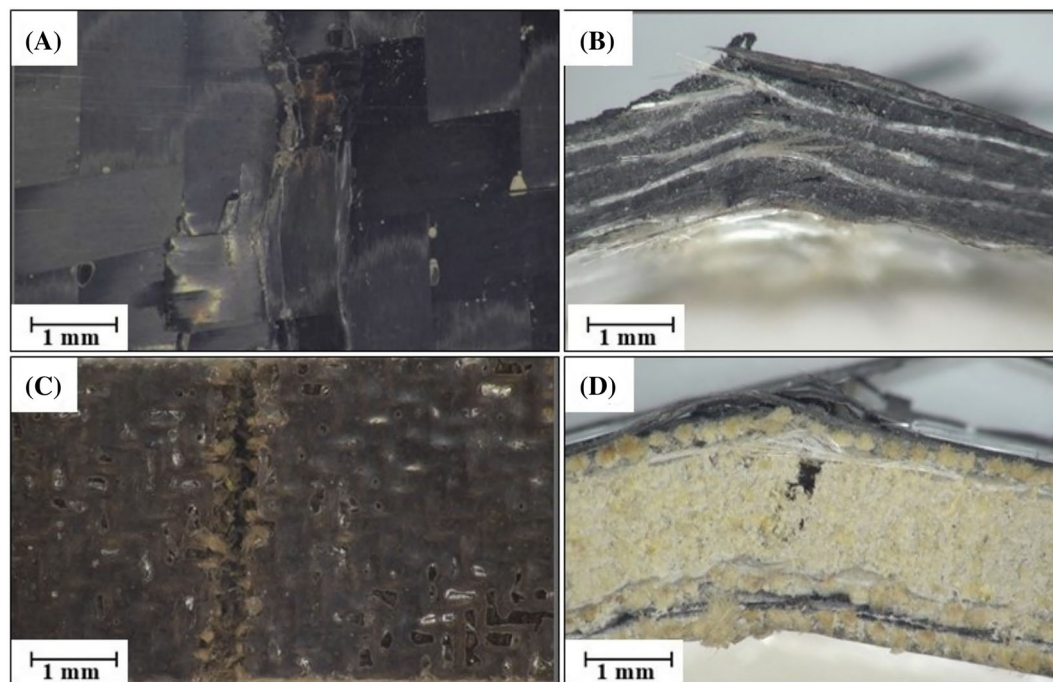


FIGURE 7 Optical microscopy of surfaces post three-point bending test of (A, B) H1 and (C, D) FH composites.

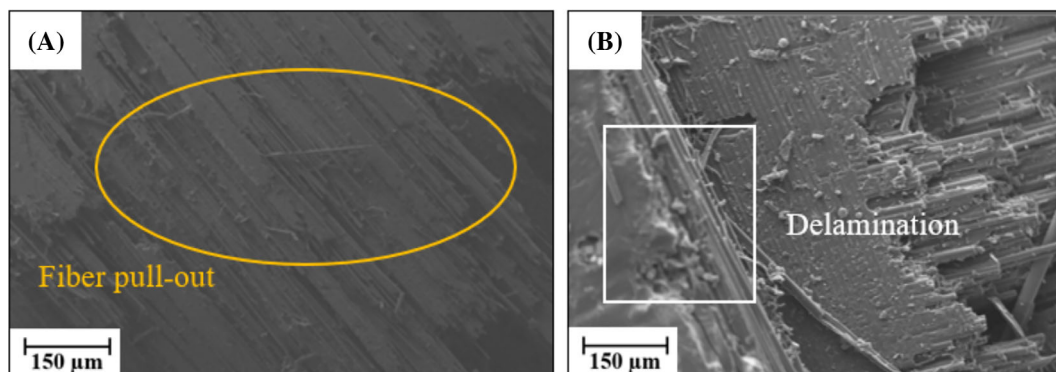


FIGURE 8 (A) Fiber pull-out and (B) Delamination on the H2 composites.

to interlaminar delamination between the GF layers. Additionally, Figure 6D shows minor fiber pull-out, which is a common failure in GF composites under bending stress that occurs due to poor bonding between the matrix and fibers. The presence of fiber pull-out on the composites suggests that the fibers absorbed energy released from matrix deformation, resulting in failure at the fiber-matrix interface, initiating multiple crack propagations within the composite.⁵⁴

The optical images presented in Figure 7 illustrate the fracture behavior of both hybrid synthetic (H1) and natural fiber (FH) composites post flexural study. The H1 composites showcased matrix cracking and significant delamination along the fiber-matrix interface, resulting in interlaminar shear failure. Furthermore, Figure 7B indicated ply delamination and localized buckling, resulting in fiber pull-out, suggesting weak interfacial bonding and the brittle nature of the H1 synthetic composites.⁵⁵ In contrast, the FH composite (Figure 7C,D) displays a more ductile fracture mechanism. The surface image (Figure 7C) reveals fiber pull-out, indicating slippage between fibers and matrix, a typical energy dissipation feature in natural fiber composites. The cross-section of the FH composites (Figure 7D) shows core material compression and delamination of the layers, suggesting the core was crushed under bending load. This highlights the material's plastic behavior before failure.

The hybrid (H2) composites made from synthetic and natural composites showcased a combination of brittle and ductile failures, as illustrated in Figure 8. It can be observed from Figure 8 that both matrix cracking and fiber pull-outs are visible in the H2 composites. Figure 8A reveals a relatively smooth fracture surface with few signs of matrix cracking, indicating a brittle failure mechanism dominated by the breakage of fibers rather than significant matrix deformation. In contrast, the partial cross-section reported in Figure 8B shows a

much rougher fracture surface characterized by extensive fiber pull-out, matrix cracking, and delamination. The presence of these features indicates a more complex failure mode under higher stress conditions, involving fiber-matrix debonding, crack propagation along fiber interfaces, and eventual fiber breakage. The combination of brittle fiber fracture and ductile matrix deformation suggests that the hybrid composite experiences mixed-mode failure, where the natural, carbon, and glass fibers each contribute differently to the overall fracture mechanics.

3.4 | Finite element approach

A finite element analysis (FEA) model was implemented using Ansys 19.2 to validate the experimental and theoretical results. The model was constructed in the static structural workbench, featuring a laminated composite structure with layers oriented at 0°. Boundary conditions for the tensile study were set to match experimental data, with one side fixed and a displacement rate of 2 mm/min applied to the opposite side. For the flexural study, based on a three-point bending method, two fixed supports were positioned with the same span length, and a load of 2 mm/min was applied to the top center of the specimen. The mesh was optimized in Ansys, resulting in an ideal element size of 0.05 mm. A tetragonal mesh with an average orthogonal quality of ~0.98 was utilized.

The theoretical values for the tensile and flexural strength were calculated using Equations (2), (3), and (4) along with the help of the rule of mixtures to evaluate the required volume and mass fractions of fibers and matrices as reported in Equations (5) and (6) where σ is the stress, ϵ is the strain, F is the force, L is the length, W is the width, D is the depth, ρ_c and E_c are the density and Young's modulus of composite, ρ_m and E_m are the density and Young's modulus of the matrix, ρ_f and E_f are

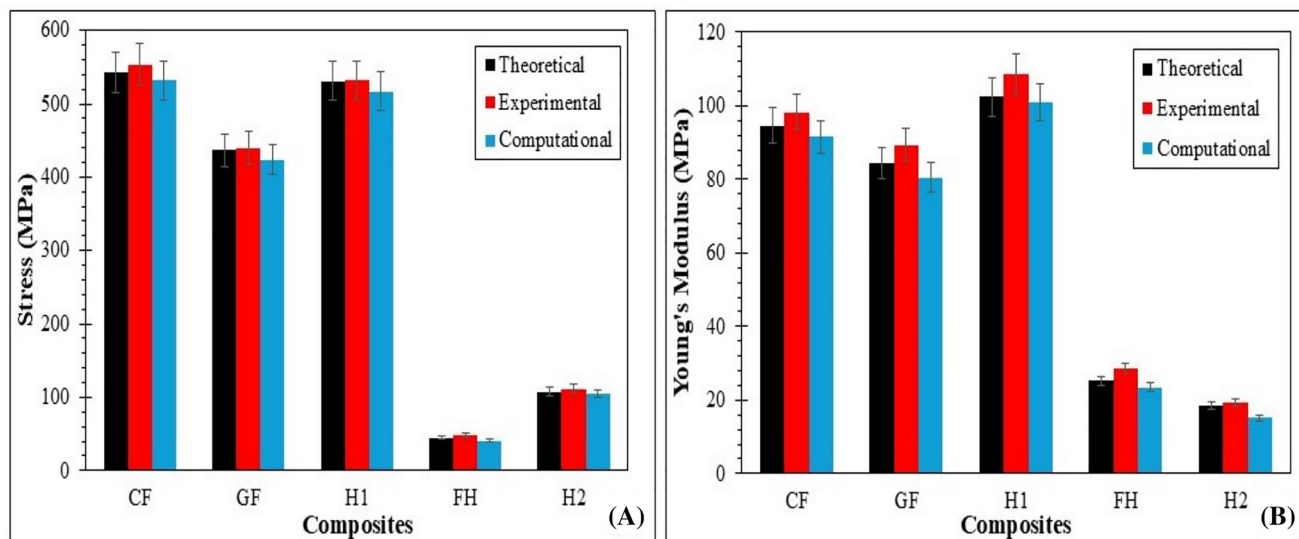


FIGURE 9 Comparison of theoretical, experimental, and computational (A) stress and (B) Young's modulus.

the density and Young's modulus of fibers, and V_f and V_m are the volume fractions of fibers and matrix.

$$\text{Stress } (\sigma) = \frac{\text{Force}}{\text{Area}} \quad (2)$$

$$E = \frac{\sigma}{\varepsilon} \quad (3)$$

$$\sigma = \frac{3FL}{2WD^2} \quad (4)$$

$$\rho_c = \rho_f V_f + \rho_m V_m \quad (5)$$

$$E_c = E_f V_f + E_m (1 - V_f) \quad (6)$$

Figure 9 provides a comprehensive comparison of theoretical, experimental, and computational data of tensile stress and Young's modulus across the composites prepared via vacuum bagging approach. From the Figure 9, it could be concluded that all the values were in closer agreement affirming the robustness of the models. These closer values also suggest that these approaches can be substituted whenever possible. In terms of tensile stress comparison reported in Figure 9A, CF demonstrates the highest strength, with theoretical predictions (~540 MPa) slightly less the experimental (~560 MPa). Likewise, similar trend was also observed on Young's modulus as reported in Figure 9B. The results demonstrate strong consistency across theoretical, experimental, and computational approaches, though minor deviations are observed in GF and H1 for Young's modulus. Overall, synthetic composites outperform hybrid and natural fiber composites in terms of stress and stiffness, while hybrid

composites achieve a compromise between strength, stiffness, and sustainability.

The discrepancies observed among computational, experimental, and theoretical values can be attributed to the inherent limitations of computational and theoretical models. Computational models often fail to capture micro-scale effects, including localized fiber-matrix interactions, and are limited by assumptions regarding boundary and loading conditions.⁵⁶ These models are also highly sensitive to the quality of input parameters, such as accurate material properties. For example, in hybrid composites, FEA tends to oversimplify critical interfacial phenomena, such as fiber debonding and pull-out, which play a vital role in load transfer. Additionally, anisotropic and non-linear behavior further challenge the accuracy of computational simulations, necessitating robust experimental validation and advanced modeling techniques. Similarly, theoretical models rely on assumptions such as material homogeneity, idealized fiber-matrix interactions, and the absence of voids or defects. These assumptions often lead to overestimations of mechanical properties, as they assume perfect fiber alignment and bonding—conditions rarely achieved in practical fabrication. The comparative results emphasize the superior mechanical performance of CF and GF composites, while hybrid systems represent a compromise, offering reduced mechanical properties but providing other design benefits such as cost-effectiveness, lightweight structures, and sustainability.

4 | CONCLUSION

This study examines the tensile and flexural behavior of synthetic composites, including glass fiber (GF) and

carbon fiber (CF), along with hybrid composites incorporating natural fibers like flax and hemp fabricated using a vacuum bagging process. CF composites exhibited the highest tensile (~550 MPa) and flexural strength (~1620 MPa), with failure modes dominated by matrix cracking and fiber breakage, due to the high stiffness and brittle nature of carbon fibers. In contrast, GF composites showed lower strength (~450 MPa) but greater ductility, attributed to fiber pull-out and matrix cracking, likely influenced by the higher strain-to-failure of glass fibers. The synthetic hybrid composites (H1) demonstrated intermediate tensile strength (~500 MPa), with a combination of CF and GF failure mechanisms. In contrast, natural fiber composites made from flax and hemp displayed lower mechanical performance (tensile strength (~150 MPa) & flexural strength (~780 MPa)) primarily due to weaker fiber-matrix interaction. The hybrid H2 composites, a mix of synthetic and natural fibers, also showed reduced strength but higher than FH composites, with failure influenced by fiber pull-out and interfacial bonding. Despite their reduced strength, hybrid composites provide a balanced mechanical performance and offer a sustainable alternative for lightweight engineering applications. This makes them particularly promising for eco-conscious designs where weight, cost, and environmental impact are critical considerations.

AUTHOR CONTRIBUTIONS

Karthikeyan Ramachandran: data curation, formal analysis, software, validation, writing – original & review drafts, visualization. **Mohammed Khan and R. A. Tharuja Perera:** formal analysis and investigation. **Doni Daniel Jayaseelan:** supervision, project administration, methodology, conceptualization, and writing – original and review drafts.

ACKNOWLEDGMENTS

Authors would like to thank Mr. Dean Wells and Mr. Simon Crust, Senior Technician, Kingston University, London, UK, for their support with experimental and characterization procedures.

CONFLICT OF INTEREST STATEMENT

The authors declare that they have no known competing financial interests or personal relationships that could have appeared to influence the work reported in this paper.

DATA AVAILABILITY STATEMENT

Data will be made available upon request.

ORCID

Karthikeyan Ramachandran  <https://orcid.org/0000-0003-2246-7309>

REFERENCES

- Soutis C. 1 – Aerospace engineering requirements in building with composites. *Polymer Composites in the Aerospace Industry (Second Edition)*. Woodhead Publishing; 2020:3-22.
- Khan F, Hossain N, Mim J, et al. Advances of composite materials in automobile applications – a review. *J Eng Res*. 2024.
- Mostafa N, Ismarrubie Z, Sapuan S, Sultan M. Effect of fabric biaxial prestress on the fatigue of woven E-glass/polyester composites. *Mater Des*. 2016;92:579-589.
- Jawaid M, Sultan M. *Sustainable Composites for Aerospace Applications*. Woodhead Publishing; 2018.
- Arockiam N, Jawaid M, Saba N. 6 – Sustainable bio composites for aircraft components. *Sustainable Composites for Aerospace Applications*. Woodhead Publishing; 2018:109-123.
- Zhang J, Lin G, Vaidya U, Wang H. Past, present and future prospective of global carbon fibre composite developments and applications. *Compos B: Eng*. 2023;250:110463.
- Elfaleh I, Abbassi F, Habibi M, et al. A comprehensive review of natural fibers and their composites: an eco-friendly alternative to conventional materials. *Res Eng Des*. 2023;19:101271.
- Andrew J, Dhakal H. Sustainable biobased composites for advanced applications: recent trends and future opportunities – a critical review. *Compos Part C: Open Access*. 2022;7:100220.
- Abotbina W, Sapuan S, Sultan M, Alkbir M, Ilyas R. Development and characterization of cornstarch-based bioplastics packaging film using a combination of different plasticizers. *Polymers*. 2021;13(20):3487.
- Mostafa N, Ismarrubie Z, Sapuan S, Sultan M. Fibre prestressed composites: theoretical and numerical modelling of unidirectional and plain-weave fibre reinforcement forms. *Compos Struct*. 2017;159:410-423.
- Palanisamy S, Vijayananth K, Murugesan T, Palaniappan M, Santulli C. The prospects of natural fiber composites: a brief review. *Int J Lightw Mater Manuf*. 2024;7(4):496-506.
- Yan L, Chou N. Crashworthiness characteristics of flax fibre reinforced epoxy tubes for energy absorption application. *Mater Des*. 2013;51:629-640.
- Agunsoye J, Aigbodion V. Bagasse filled recycled polyethylene bio-composites: morphological and mechanical properties study. *Results Phys*. 2013;3:187-194.
- Gurunathan T, Mohanty S, Nayak S. A review of the recent developments in biocomposites based on natural fibres and their application perspectives. *Compos Part A: Appl Sci Manuf*. 2015;77:1-25.
- Safri S, Sultan M, Jawaid M, Jayakrishna K. Impact behaviour of hybrid composites for structural applications: a review. *Compos B: Eng*. 2018;133:112-121.
- Chen L, Msigwa G, Yang M, et al. Strategies to achieve a carbon neutral society: a review. *Environ Chem Lett*. 2022;20:2277-2310.
- Ramachandran K, Gnanasagaran C. Life cycle assessment of sugarcane bagasse based natural composites prepared via vacuum bagging technique. *Bioresour Technol Rep*. 2024;26:101811.
- Phiri R, Rangappa S, Siengchin S, Oladijo O, Dhakal H. Development of sustainable biopolymer-based composites for lightweight applications from agricultural waste biomass: a review. *Adv Ind Eng Polym Res*. 2023;6(4):436-450.

19. Akhil U, Radhika N, Saleh B, Krishna S, Novel N, Rajeshkumar L. A comprehensive review on plant-based natural fiber reinforced polymer composites: fabrication, properties, and applications. *Polym Compos.* 2023;44(5):2598-2633.
20. Fan Q, Duan H, Xing X. A review of composite materials for enhancing support, flexibility and strength in exercise. *Alex Eng J.* 2024;94:90-103.
21. Khandelwal S, Rhee K. Recent advances in basalt-fiber-reinforced composites: tailoring the fiber-matrix interface. *Compos B: Eng.* 2020;192:108011.
22. Karimah A, Ridho M, Munawar S, et al. A review on natural fibers for development of eco-friendly bio-composite: characteristics, and utilizations. *J Mater Res Technol.* 2021;13:2442-2458.
23. Ramachandran K, Gnanasagaran C, Vekariya A. Life cycle assessment of carbon fiber and bio-fiber composites prepared via vacuum bagging technique. *J Manuf Process.* 2023;89:124-131.
24. Ramesh M, Palanikumar K, Reddy K. Plant fibre based bio-composites: sustainable and renewable green materials. *Renew Sust Energ Rev.* 2017;79:558-584.
25. Zuo P, Srinivasan D, Vassilopoulos A. Review of hybrid composites fatigue. *Compos Struct.* 2021;274:114358.
26. Kim E, Ahn C, Yu W, Na W. Influence of water absorption on the interlaminar behavior of carbon fiber-reinforced composites containing halloysite nanotubes. *Compos Part A: Appl Sci Manuf.* 2023;175:107811.
27. Aranha R, Filho M, Santos C, et al. Effect of water absorption and stacking sequences on the tensile properties and damage mechanisms of hybrid polyester/glass/jute composites. *Polymers.* 2024;16(7):925.
28. Venkateshwaran N, Elayaperumal A, Alavudeen A, Thiruchitrabalam M. Mechanical and water absorption behaviour of banana/sisal reinforced hybrid composites. *Mater Des.* 2011;32(7):4017-4021.
29. Jesthi D, Nayak R. Improvement of mechanical properties of hybrid composites through interply rearrangement of glass and carbon woven fabrics for marine application. *Compos B: Eng.* 2019;168:467-475.
30. Zafar A, Bertocco F, S-Thomsen J, Rauhe J. Investigation of the long term effects of moisture on carbon fibre and epoxy matrix composites. *Compos Sci Technol.* 2012;72(6):656-666.
31. Sari N, Sujita S, Anshari B, Syafr E, Achaby M, Slitonga A. Exploring the impact of water soaking on the mechanical, thermal, and physical properties of *Paederia foetida* fiber stem bio-composites: a study in sustainable material innovation. *Case Stud Chem Environ Eng.* 2024;10:100977.
32. Munimathan A, Muthu K, Subramani S, Rajendran S. Environmental behaviour of synthetic and natural fibre reinforced composites: a review. *Adv Mech Eng.* 2024;16(10):16878132241286020. doi:10.1177/16878132241286020
33. Gao H, Sun Y, Jian J, Dong Y, Liu H. Study on mechanical properties and application in communication pole line engineering of glass fiber reinforced polyurethane composites (GFRP). *Case Stud Constr Mater.* 2023;18:e01942.
34. Ning N, Wang M, Zhou G, Qiu Y, Wei Y. Effect of polymer nanoparticle morphology on fracture toughness enhancement of carbon fiber reinforced epoxy composites. *Compos B: Eng.* 2022;234:109749.
35. Beier U, Fischer F, Sandler J, Altstadt V, Weimer C, Buchs W. Mechanical performance of carbon fibre-reinforced composites based on stitched preforms. *Compos Part A: Appl Sci Manuf.* 2007;38(7):1655-1663.
36. Fallahi H, Kaynan O, Asadi A. Insights into the effect of fiber-matrix interphase physiochemical- mechanical properties on delamination resistance and fracture toughness of hybrid composites. *Compos Part A: Appl Sci Manuf.* 2023;166:107390.
37. Sathishkumar T, Naveen J, Satheeshkumar S. Hybrid fiber reinforced polymer composites – a review. *J Reinf Plast Compos.* 2014;33(5):454-471.
38. Vedrtnam A, Sharma S. Study on the performance of different nano-species used for surface modification of carbon fiber for interface strengthening. *Compos Part A: Appl Sci Manuf.* 2019;125:105509.
39. Ramachandran K, Azadani M, Ravichandran P, Shivaprakash N, Obi M, Gnanasagaran C. Failure mechanics of fused filament fabricated nylon/carbon-reinforced composites. *Prog Addit Manuf.* 2024;9:2089-2097.
40. Dhand V, Mittal G, Rhee K, Park S, Hui D. A short review on basalt fiber reinforced polymer composites. *Compos B: Eng.* 2015;73:166-180.
41. Akshita T, Gupta D, Gupta N, Chandel S, Kumar R, Choubey R. Glass fiber-reinforced polymer composites. *Polymer Composites: Fundamentals and Applications.* Springer; 2024:181-216.
42. Kusmono TA, Herianto MW. Mechanical, morphological, and thermal characteristics of epoxy/glass fiber/cellulose nanofiber hybrid composites. *Polym Test.* 2022;110:107560.
43. Ikbali H, Wang Q, Azzam A, Li W. Effect of hybrid ratio and laminate geometry on compressive properties of carbon/glass hybrid composites. *Fibers Polym.* 2016;17:117-129.
44. Maiti S, Islam M, Uddin M, Afroj S, Eichhorn S, Karim N. Sustainable fiber-reinforced composites: a review. *Adv Sustain Syst.* 2022;6(11):1-33.
45. Vega E d, Allegri G, Zhang B, Hamerton I, Hallett S. Pseudoductile behaviour of fibrous composite Z-pins. *Compos Part A: Appl Sci Manuf.* 2024;178:108009.
46. Norman D, Robertson R. The effect of fiber orientation on the toughening of short fiber-reinforced polymers. *J Appl Polym Sci.* 2003;90(10):2740-2751.
47. Feng Y, Hao H, Lu H, Chow C, Lau D. Exploring the development and applications of sustainable natural fiber composites: a review from a nanoscale perspective. *Compos B: Eng.* 2024;276:111369.
48. Haris N, Hassan M, Ilyas R, et al. Dynamic mechanical properties of natural fiber reinforced hybrid polymer composites: a review. *J Mater Res Technol.* 2022;19:167-182.
49. Rajak D, Wagh P, Linul E. A review on synthetic fibers for polymer matrix composites: performance, failure modes and applications. *Materials.* 2022;15(4):4790.
50. Peltola H, Madsen B, Joffe R, Nattinen K. Experimental study of fiber length and orientation in injection molded natural fiber/starch acetate composites. *Adv Mater Sci Eng.* 2011;2011(1):1-7.
51. Patou J, Bonnaire R, Luycker E, Bernhart G. Influence of consolidation process on voids and mechanical properties of powdered and commingled carbon/PPS laminates. *Compos Part A: Appl Sci Manuf.* 2019;117:260-275.

52. Alam P, Mamalis D, Robert C, Folreani C, Bradaigh C. The fatigue of carbon fibre reinforced plastics – a review. *Compos B: Eng.* 2019;166:555-579.
53. Huang S, Fu Q, Yan L, Kasal B. Characterization of interfacial properties between fibre and polymer matrix in composite materials – a critical review. *J Mater Res Technol.* 2021;13:1441-1484.
54. Li L, Ma Z, Xu P, et al. Flexible and alternant-layered cellulose nanofiber/graphene film with superior thermal conductivity and efficient electromagnetic interference shielding. *Compos Part A: Appl Sci Manuf.* 2020;139:106134.
55. Boon U, Joshi S. A review of methods for improving interlaminar interfaces and fracture toughness of laminated composites. *Mater Today Commun.* 2020;22:100830.
56. Ramachandran K, Soni A, Jayaseelan D. Investigating the impact of notch shapes on oxide-oxide CMCs strength: a computational approach. *Int J Ceram Eng Sci.* 2024;6(6):1-11.

How to cite this article: Ramachandran K, Khan M, Tharuja Perera RA, Daniel Jayaseelan D. Tensile and flexural behavior of synthetic and hybrid natural fiber composites for lightweight applications. *Polym Compos.* 2025;1-13. doi:[10.1002/pc.29781](https://doi.org/10.1002/pc.29781)